ELSEVIER

Journal of Organometallic Chemistry 680 (2003) 193–205

Journal of Organometallic Chemistry

www.elsevier.com/locate/jorganchem

Ansa-metallocenes with B–N and B–P linkages: the importance of N–H···F–C hydrogen bonding in pentafluorophenyl boron compounds

Simon J. Lancaster *, Andrew J. Mountford, David L. Hughes, Mark Schormann, Manfred Bochmann *

Wolfson Materials and Catalysis Centre, School of Chemical Sciences and Pharmacy, University of East Anglia, Norwich NR4 7TJ, UK

Received 19 March 2003; received in revised form 23 April 2003; accepted 23 April 2003

Dedicated to Professor M.F. Hawthorne on the occasion of his 75th birthday

Abstract

The reaction of $Cp'(Cp^B)ZrCl_2$ [$Cp^B = \eta^5$-$C_5H_4B(C_6F_5)_2$] with $LiNHCMe_3$ gave $Cp'(Cp^B)(\mu$-$NHCMe_3)ZrCl$, with a constrained-geometry type Cp–B–N chelate ligand. The ^{19}F-NMR spectrum of the zirconium complexes, as well as that of the titanium analogue, reveals C–F···H–N hydrogen bonding to one of the *ortho*-F atoms of a C_6F_5 ring, strong enough to persist in solution at room temperature. The reaction of $Cp'(Cp^B)TiCl_2$ with $LiPPh_2$ affords the Cp–B–P chelate complex $Cp'(Cp^B)(\mu$-$PPh_2)TiCl$, the first example of a crystallographically characterised Ti(IV) phosphido compound. A ^{19}F-NMR study of a number of adducts of $B(C_6F_5)_3$ with *prim*- and *sec*-amines demonstrates the importance of intramolecular hydrogen bonding to C_6F_5 in this class of compounds, while there are no such interactions in $B(C_6F_5)_3(PHR_2)$ (R = Cy, Ph). The crystal structures of $Cp'(Cp^B)(\mu$-$PPh_2)TiCl$, $B(C_6F_5)_3(NHMe_2)$ and $B(C_6F_5)_3(PHCy_2)$ are reported.

Keywords: *Ansa*-metallocenes; Boron; Hydrogen bonding; Heteroatom bridges; Amido complexes; Phosphido complexes

1. Introduction

We recently reported the synthesis of Group 4 cyclopentadienyl complexes bearing Lewis acidic bis(pentafluorophenyl)boryl substituents and their behaviour as self-activating alkene polymerisation catalysts [1]. In titanium complexes the boryl substituents were found to activate chloro ligands, depending on the Cp^B–Ti–Cl angle [2]. Reetz reported the preparation of the first boryl zirconocenes through the dehalosilylation reaction between $ZrCl_4$ or $CpZrCl_3$ and $C_5H_4(SiMe_3)BX_2$ (X = Me, Et, OEt and C_6F_5 (**I**, Chart 1)) [3]. Titanocenes with boryl-cyclopentadienyl ligands, $Cp'(Cp^B)TiCl_2$ ($Cp^B = \eta^5$-$C_5H_4B(C_6F_5)_2$, $Cp' = C_5H_5$ (**II**), C_9H_7, $C_5H_4SiMe_3$), are accessible by reacting $(Cp^B)TiCl_3$ with LiCp′ [4]. This route has recently been extended to zirconocenes [5].

The bonding in this type of complexes is a fine balance of steric factors. For example, whereas $(Cp^B)(Ind)TiCl_2$ has a crystallographically characterised Cp–B–Cl–Ti linkage, there is no such B–Cl interaction in the zirconium analogues $Cp'(Cp^B)ZrCl_2$ ($Cp' = C_5H_5$ and C_9H_7), which, unlike the titanocenes, readily form adducts between weak bases such as Me_2S and boron (**III**) [5]. The steric relief in going from titanium to zirconium means that the Cp–B–Cl–Zr interaction is not favoured.

Our initial studies on the interaction of titanium complexes with boryl-Cp ligands demonstrated that the Cp–B–N–Ti linkage was preferred over Cp–B–Cl–Ti. Here we report several complexes of the type $Cp(Cp^B)M(Cl)(\mu$-NHR) (M = Ti, Zr) which display Cp–B–N ‘constrained geometry’ bonding, as well as examples of related compounds with Cp–B–P linkages.

---

* Corresponding authors. Tel./fax: +44-1603-59-2009.

E-mail addresses: s.lancaster@uea.ac.uk (S.J. Lancaster), m.bochmann@uea.ac.uk (M. Bochmann).

0022-328X/03/$ - see front matter © 2003 Elsevier Science B.V. All rights reserved.
doi:10.1016/S0022-328X(03)00346-2

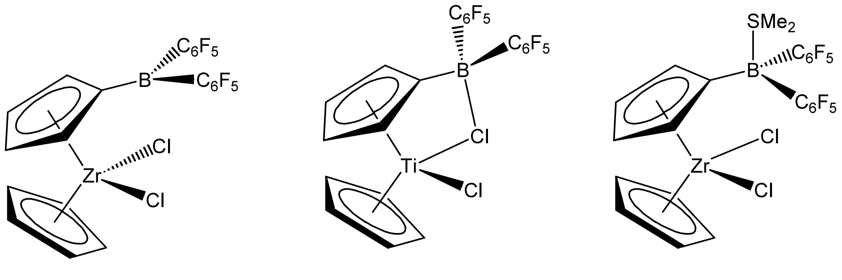

I **II** **III**

Plate 1.

A more detailed structural investigation revealed the importance of N–H···F–C hydrogen bonding, a feature that has also been found to be prominent in adducts of $B(C_6F_5)_3$ with amines. Dunitz and Taylor, in their statistical analysis of crystallographic data, have pointed out that 'organic fluorine hardly ever accepts hydrogen bonds' [6]. Nevertheless, in biological chemistry OH··· F–C and NH···F–C interactions are considered important for the binding of fluorinated substrates to enzymes [7], even if this notion has been somewhat controversial [8]. A number of complexes of perfluoroaryl boranes with amines and phosphines have therefore been included in this study.

2. Results and discussion

Following the procedure we developed for the preparation of $Cp(Cp^B)TiCl(NHCMe_3)$ (**1**), the reaction of $Cp(Cp^B)ZrCl_2(SMe_2)$ with one equivalent of $LiNHCMe_3$ resulted in the analogous zirconium complex **2** (Scheme 1). The ^1H- and ^{11}B-NMR resonances were almost identical to those of **1** (Table 1). The room temperature ^{19}F-NMR spectrum of **2** (Fig. 1) was more complex than anticipated, with a separate resonance for each of the ten fluorine nuclei in the molecule. Evidently rotation of the two chemically inequivalent $B–C_6F_5$ moieties is strongly hindered. There are four *o*-F resonances, one of which, at δ −142.6, shows a significant high-field shift from the normal *o*-F region. Prompted by this observation, we recorded the ^{19}F-NMR spectrum of the titanium complex **1**, which proved to be very similar. The explanation for this unusual ^{19}F signal was apparent on re-examination of the solid-state structure of **1** which showed a previously unrecognised N–H···F interaction, with a short H···F distance of 2.11 Å and a wide N–H–F angle of 147°. High-field *o*-F shifts have been reported for compounds with Zr···F contacts [9,10], as well as for the anion $[NH_2\{B(C_6F_5)_3\}_2]^-$ which provided crystallographic evidence for a range of N–H···F interactions [11].

Dunitz et al. have laid down criteria for such interactions, i.e. the H···F–C interaction should be significantly shorter than the sum of the van der Waals radii (ca. 2.55 Å) and preferably be no longer than ca. 2.2–2.3 Å, with obtuse H–F–C angles [6]. The NH···F interactions in the μ-NH_2 diborate anion $[NH_2\{B(C_6F_5)_3\}_2]^-$ range from 1.90 to 2.43 Å (Fig. 2) [11]. This was reflected in its solution behaviour where at −90 °C only one of the six C_6F_5 substituents was found to rotate freely, although there was no evidence for hindered rotation on the NMR timescale at room temperature. Complexes **1** and **2** have similar intramolecular N–H···F–C hydrogen bonds; however, in these cases they prevent free rotation in solution even at room temperature. Indeed, the N–H···F–C bonding in **2** is

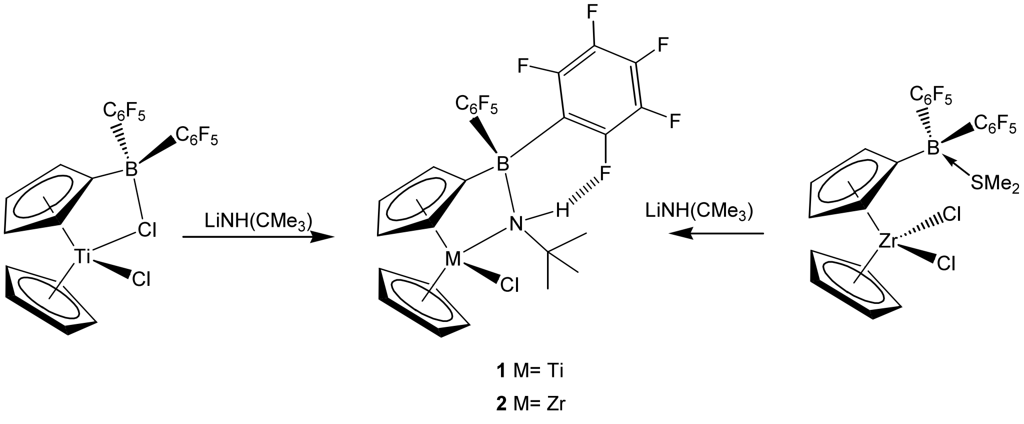

1 M= Ti
2 M= Zr

Scheme 1.

Table 1
Multinuclear NMR data of pentafluorophenyl boron compounds

Multinuclear NMR data of pentafluorophenyl boron compounds.	
Cp(Cp^B)Ti(Cl)(NCMe$_3$H) (**1**) 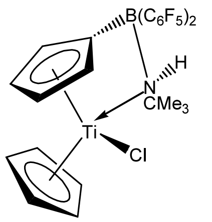	δ_H (300 MHz, C_6D_6, 20°C) 7.08-7.04 (m, 1H, C_5H_4), 6.39-6.35 (m, 1H, C_5H_4), 5.60 (s, 5H, Cp), 5.28-5.26 (m, 1H, C_5H_4), 5.19-5.17 (br, 1H, C_5H_4), 3.15 (d, 1H, *J*(HF) 20 Hz, N*H*^{t}Bu), 1.09 (s, 9H, NH^t*Bu*) δ_C (75.47 MHz; C_6D_6, 20°C) 134.57 (C_5H_4), 131.64 (C_5H_4), 121.16 (Cp), 117.87 (C_5H_4), 114.93 (C_5H_4), 56.52 (*C*(CH_3)$_3$), 30.50 (C(*C*H_3)$_3$) δ_B (96.29 MHz, C_6D_6, 20°C) -8.2 δ_F (282.40 MHz, C_6D_6, 20°C) -123.61 (d, 1F, *J*(FF) 24 Hz, *o*-F), -126.41 (d, 1F, *J*(FF) 19 Hz, *o*-F), -129.66 (d, 1F, *J*(FF) 24 Hz, *o*-F), -141.56 (m, 1F, *o*-F), -155.90 (t, 1F, *J*(FF) 21 Hz, *p*-F), -157.54 (t, 1F, *J*(FF) 21 Hz, *p*-F), -161.72 (t, 1F, *J*(FF) 22 Hz, *m*-F), -163.83 (t, 1F, *J*(FF) 22 Hz, *m*-F), -164.28 (t, 1F, *J*(FF) 22 Hz, *m*-F), -164.55 (t, 1F, *J*(FF) 20 Hz, *m*-F)
Cp(Cp^B)Zr(Cl)(NCMe$_3$H) (**2**) 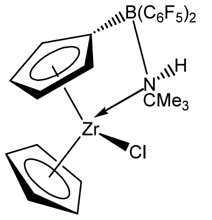	δ_H (300 MHz, C_6D_6, 20°C) 6.75-6.71 (m, 1H, C_5H_4), 6.54-6.51 (m, 1H, C_5H_4), 5.62 (s, 5H, Cp), 5.28-5.26 (m, 1H, C_5H_4), 5.02 (br, 1H, C_5H_4), 3.14 (d, 1H, *J*(HF) 22.3 Hz, N*H*^{t}Bu), 1.01 (s, 9H, NH^t*Bu*) δ_C (75.47 MHz; C_6D_6, 20°C) 131.38 (C_5H_4), 124.86 (C_5H_4), 116.71 (C_5H_4), 114.97 (Cp) 109.88 (C_5H_4), 55.52 (*C*(CH_3)$_3$), 31.12 (C(*C*H_3)$_3$) δ_B (96.29 MHz, C_6D_6, 20°C) -5.0 δ_F (282.40 MHz, C_6D_6, 20°C) -124.25 (d, 1F, *J*(FF) 24 Hz, *o*-F), -125.76 (d, 1F, *J*(FF) 19 Hz, *o*-F), -129.42 (d , 1F, *J*(FF) 24 Hz, *o*-F), -142.57 (m, 1F, *o*-F), -155.98 (t, 1F, *J*(FF) 21 Hz, *p*-F), -157.52 (t, 1F, *J*(FF) 21 Hz, *p*-F), -161.70 (t, 1F, *J*(FF) 23 Hz, *m*-F), -163.62 (t, 1F, *J*(FF) 22 Hz, *m*-F), -164.44 70 (t, 1F, *J*(FF) 24 Hz, *m*-F), -164.82 70 (t, 1F, *J*(FF) 24 Hz, *m*-F)
Cp(Cp^B)Ti(Cl)(NH$_2$) (**3**)	δ_H (300 MHz, C_6D_6, 20°C) 6.87 (br, 1H, C_5H_4), 5.90-5.88 (m, 1H, C_5H_4), 5.58-5.56 (m, 1H, C_5H_4), 5.54 (s, 5H, Cp), 5.27 (br, 1H, C_5H_4), 2.52 (br, 1H, TiN*H*$_2$), -0.21 (br, 1H, TiN*H*$_2$) δ_C (75.47 MHz; C_6D_6, 20°C) 130.82 (C_5H_4), 128 (C_5H_4), 119.30 (C_5H_4), 118.24 (Cp), 116.72 (C_5H_4) δ_B (96.29 MHz, C_6D_6, 20°C) -6.3

Table 1 (*Continued*)

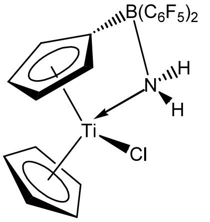	δ_F (282.40 MHz, C_6D_6, 20°C) -134.10 (d, 2F, *J*(FF) 20 Hz, *o*-F), -134.48 (br, 2F, *o*-F), -157.71 (t, 1F, *J*(FF) 21 Hz, *p*-F), -157.83 (t, 1F, *J*(FF) 20 Hz, *p*-F), -163.00 (t, 2F, *J*(FF) 20 Hz, *m*-F), -163.47 (t, 2F, *J*(FF) 20 Hz, *m*-F)
$Cp(Cp^B)Ti(Cl)(PPh_2)$ (**4**) 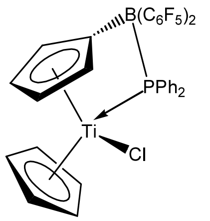	δ_H (300 MHz, C_6D_6, 20°C) 7.17 (m, 10H, Ph), 6.70 (s, 1H, Cp^B), 6.54 (m, 1H, Cp^B), 6.33 (m, 5H, Cp), 5.70 (m, 1H, Cp^B), 5.32 (m, 1H, Cp^B) δ_C (75.47 MHz; C_6D_6, 20°C) 137.1, 136.9, 135.9 (d, *J* = 8.3 Hz), 133.7 (d, *J* = 6.6 Hz), 129.6 (dd, *J* = 23.8 Hz), 128.4 (dd, *J* = 15.1 and 8.6 Hz), 122.1, 119.7, 117.7, 116.8, 116.2 δ_B (96.29 MHz, C_6D_6, 20°C) -8.9 δ_P (121.50 MHz, C_6D_6, 20°C) -67.7 δ_F (282.40 MHz, C_6D_6, 20°C) -121.41 (d, 2F *J* = 19.8 Hz, *o*-F), -123.15 (d, 2F *J* = 19.8 Hz, *o*-F), -153.64 (t, 1F *J* = 19.8 Hz, *p*-F), -154.38 (t, 1F *J* = 19.8 Hz, *p*-F), -159.5 (m, 2F *m*-F), -160.26 (m, 2F *m*-F)
$(C_6F_5)_3B(NH_2CMe_3)$ (**5**)	δ_H (300 MHz, $C_6D_5CD_3$, 20°C): 4.29 (br, 2H $\mathrm{N}\mathit{H}_2$), 0.50 (s, 9H, $\mathrm{NC}(\mathit{CH}_3)_3$) δ_C (75.47 MHz; $C_6D_5CD_3$, 20°C): 57.6 ($\mathrm{N}\mathit{C}(\mathrm{CH}_3)_3$), 28.1 $\mathrm{NC}(\mathit{CH}_3)_3$ δ_B (96.29 MHz, $C_6D_5CD_3$, 20°C): -5.2 δ_F (282.40 MHz, $C_6D_5CD_3$, 20°C): -132.6 (br, 6F, *o*-F), -155.7 (br, 3F, *p*-F), -162.8 (br, 6F, *m*-F) δ_F (282.40 MHz, $C_6D_5CD_3$, -60°C): -129.3 (br, 1F, *o*-F), -130.0 (br, 1F, *o*-F), -131.5 (br, 2F *o*-F), -134.9 (br, 1F *o*-F), -137.9 (br, 1F *o*-F), -153.9 (br, 1F, *p*-F), -155.5 (br, 1F, *p*-F), -161.2 (br, 2F, *m*-F), -162.7 (br, 2F, *m*-F), -164.5 (br, 2F, *m*-F)
$(C_6F_5)_3B(NHMe_2)$ (**6**)	δ_H (300 MHz, C_6D_6, 20°C) 6.23 (broad s, 1H, NH), 2.62 (d, 6H, *J* 5.4 Hz, CH_3) δ_C (75.47 MHz; C_6D_6, 20°C) 40.05 (2C, s, CH_3) δ_B (96.29 MHz, C_6D_6, 20°C) -1.4 δ_F (282.40 MHz, C_6D_6, 20°C) -127.62 (m, 2F, *o*-F), -128.26 (m, 2F, *o*-F), -142.24 (m, 2F, *o*-F), -154.51 (m, 1F, *p*-F), -156.74 (m, 1F, *p*-

Table 1 (*Continued*)

	F), -161.31 (m, 2F, *m*-F), -162.86 (m, 4F, *m*-F)
(Flu)B$(C_6F_5)_2(NH_2CMe_3)$ (**7**) 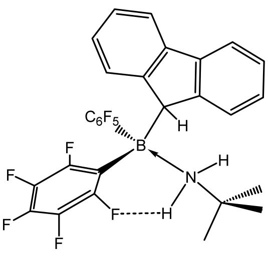 	δ_H (300 MHz, $CDCl_3$, 20°C): 7.84 (d, 2H, *J* = 8Hz, Flu), 7.67 (d, 2H, *J* = 7 Hz, Flu), 7.53 (m, 4H, Flu), 5.16 (br, 2H, NH_2), 4.84 (s, 1H, BC*H*), 1.65 (s, 9H, $C(CH_3)_3$) δ_C (75.47 MHz; $CDCl_3$, 20°C): 148.7, 141.7, 126.0, 125.8, 123.8, 119.5 7 (Flu), 58.0 ($C(CH_3)_3$), 47.0 (B*C*H), 30.0 ($C(CH_3)_3$) δ_B (96.29 MHz, $CDCl_3$, 20°C): -4.2 δ_F (282.40 MHz, $C_6D_5CD_3$, 20°C): -127.05 (br, 4F, *o*-F), -157.1 (br, 2F, *p*-F), -164.06 (br, 4F, *m*-F) δ_F (282.40 MHz, $C_6D_5CD_3$, -40°C): -124.63 (d, 1F *J* = 19.8 Hz, *o*-F), -127.19 (d, 1F *J* = 25.4 Hz, *o*-F), -130.48 (d, 1F *J* = 22.6 Hz, *o*-F), -134.18 (d, 1F *J* = 25.4 Hz, *o*-F), -154.36 (tr, 1F *J* = 19.8 Hz, *p*-F), -158.07 (tr, 1F *J* = 22.6 Hz, *p*-F), -162.07 (tr, 1F *J* = 19.8 Hz, *m*-F), -162.59 (tr, 1F *J* = 19.8 Hz, *m*-F), -164.17 (tr, 1F *J* = 22.6 Hz, *m*-F), -165.90 (tr, 1F *J* = 22.6 Hz, *m*-F)
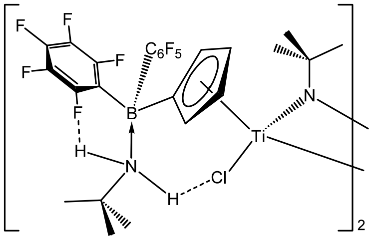 (**8**)	δ_H (300 MHz, $CDCl_3$, 20°C): 7.04 (tr, 2H, *J* = 2.6 Hz, C_5H_4B), 5.78 (br, 2H, C_5H_4B), 1.19 (s, 9H, μ-$NC(CH_3)_3$), 0.93 (s, 9H, B-$NC(CH_3)_3$) δ_C (75.47 MHz; $CDCl_3$, 20°C): 125.6, 121.3 (C_5H_4B), 77.8 (μ-N$C(CH_3)_3$), 56.9 (B-N$C(CH_3)_3$), 33.8 (μ-$NC(CH_3)_3$), 29.4 (B-$NC(CH_3)_3$) δ_B (96.29 MHz, $CDCl_3$, 20°C): -5.0 δ_F (282.40 MHz, $C_6D_5CD_3$, 20°C): -128.53 (br, 8F, *o*-F), -156.99 (br, 4F, *p*-F), -163.59 (br, 8F, *m*-F)
(Ind)B$(C_6F_5)_2(NH_2CMe_3)$ (**9**)	δ_H (300 MHz, $CDCl_3$, 20°C): 7.48-7.45 (m, 1H, Ind), 7.16-7.06 (m, 3H, Ind), 6.36 (s, 2H, Ind), 4.93 (br s, 2H, NH_2), 3.37 (s, 2H, Ind-CH_2). 1.27 (s, 9H, $C(CH_3)_3$) δ_C (75.47 MHz; $CDCl_3$, 20°C): 148.3, 145.0, 134.2, 126.1, 124.0, 123.8, 121.0 (Ind), 57.3 ($C(CH_3)_3$), 39.7 (Ind-CH_2), 29.6 ($C(CH_3)_3$) δ_B (96.29 MHz, $CDCl_3$, 20°C): -7.6 δ_F (282.40 MHz, $C_6D_5CD_3$, 20°C): -130.36 (br, 4F, *o*-F), -157.20 (br, 2F, *p*-F), -163.43 (br, 4F, *m*-F)
$(C_6F_5)_3B(PHCy_2)$ (**10**)	δ_H (300 MHz, C_6D_6, 20°C) 5.20 (dt, 1H, *J*(HP) 405.5 Hz and *J*(HH) 4.4 Hz, PH), 1.95-1.30 (m, 22H, C_6H_{11}) δ_C (75.47 MHz; C_6D_6, 20°C) 31.23 (C_6H_{11}), 30.97 (C_6H_{11}), 30.57 (C_6H_{11}), 30.23 (C_6H_{11}), 30.15 (C_6H_{11}), 27.22 (C_6H_{11}), 27.07 (C_6H_{11}),

Table 1 (*Continued*)

	26.65 (C_6H_{11}), 26.51 (C_6H_{11}) δ_B (96.29 MHz, C_6D_6, 20°C) -13.5 (d, *J*(BP) 64.0 Hz) δ_P (121.50 MHz, C_6D_6, 20°C) 9.29 (d, *J* 76.42 Hz) δ_F (282.40 MHz, C_6D_6, 20°C) -129.85 (*o*-F), -156.71 (t, 3F, *J* 22.6 Hz, *p*-F), -163.06 (t, 6F, *J* 15 Hz, *m*-F)
$(C_6F_5)_3B(PHPh_2)$ (**11**)	δ_H (300 MHz, C_6D_6, 20°C) 7.11-6.80 (m, 10H, C_6H_5), 6.68 (d, 1H, *J*(PH) 411.2 Hz, PH) δ_C (75.47 MHz; C_6D_6, 20°C) 133.76 (d, 2C, *J* 8.2 Hz, C_6F_5), 132.68 (d, 2C, *J* 2.7 Hz, C_6F_5), 129.32 (d, 2C, *J* 10.7 Hz, C_6F_5), 121.75 (d, 2C, *J* 57.7 Hz, C_6F_5) δ_B (96.29 MHz, C_6D_6, 20°C) -9.4 δ_P (121.50 MHz, C_6D_6, 20°C) 0.88 δ_F (282.40 MHz, C_6D_6, 20°C) -128.45 (s, 6F, *o*-F), -156.10 (s, 3F, *p*-F), -163.32 (s, 6F, *m*-F)

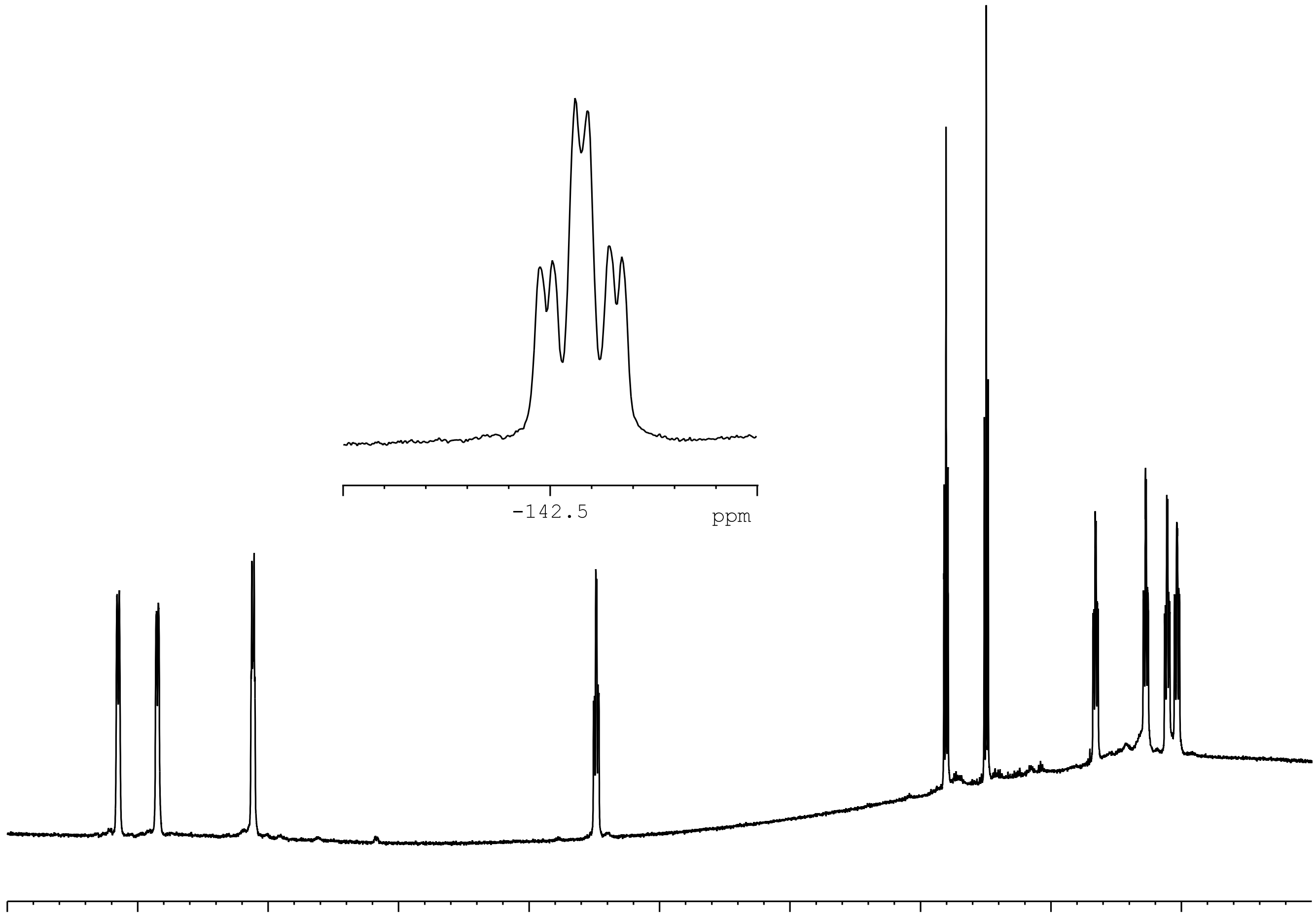

Fig. 1. ^{19}F-NMR spectrum of the zirconium complex **2** at 25 °C. The high-field *o*-F signal at δ −142.6 is indicative of hydrogen bonding to N–H.

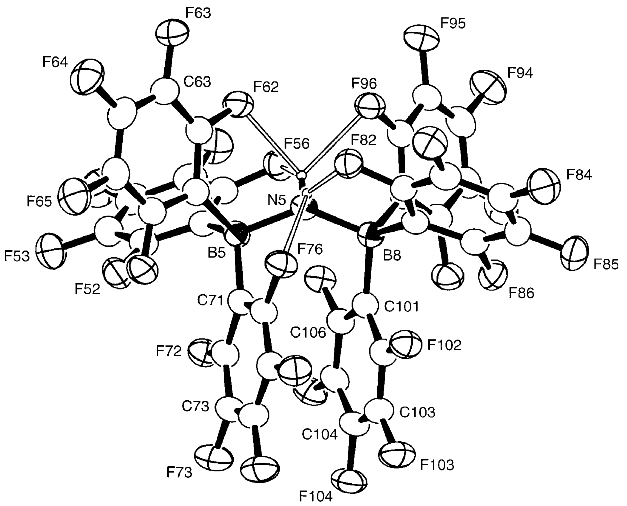

Fig. 2. Structure of the anion $[NH_2\{B(C_6F_5)_3\}_2]^-$, illustrating the C–F···HN hydrogen-bonding pattern [11].

sufficiently rigid to show N–H···F fluorine coupling in the ^{1}H-NMR spectrum at 25 °C (δ 3.13, $J_{HF} = 22.3$ Hz).

Efforts were made to extend the synthesis of Cp–B–N constrained geometry-type systems to the parent NH_2 linkage. Because of the low solubility of $NaNH_2$, the reaction with $Cp^BCpTiCl_2$ required the use of tetrahydrofuran as the solvent and extended reaction times. Over 36 h the sodium amide dissolved and a bright red solution of $Cp(Cp^B)Ti(NH_2)Cl$ (**3**) was formed (Scheme 2). Attempts to grow crystals suitable for X-ray diffraction were not successful; however, the structure represented in Scheme 2 is consistent with the elemental analysis and spectroscopic data. The ^{1}H-NMR spectrum shows signals for four inequivalent protons of the C_5H_4B ring. The NH_2 group is diastereotopic, although the coupling is obscured by line-broadening. In addition, the ^{11}B-NMR resonance, δ −6.3, indicates a tetrahedral coordination environment. The data suggest Cp–B–N–Ti bonding, as in **1**. The case for a N–H···F–C hydrogen bonding interaction in this complex is less clear-cut since, although the two C_6F_5 groups are inequivalent at room temperature, no high field *o*-F resonance is observed. Poor solubility precluded a low-temperature study.

Having successfully prepared examples with ‘constrained geometry’ *ansa*-cyclopentadienyl-amido Cp–B–N–M bonding we wished to determine whether the analogous phosphido complexes would adopt a similar Cp–B–P–M structure. *Ansa*-cyclopentadienyl phosphido complexes with a bridging carbon or silicon atom have recently been prepared by Erker and coworkers [12]. The first fully characterised mononuclear metallocene(IV) diphosphides, $Cp_2M(PR_2)_2$ (M = Zr, Hf; R = Ph, Cy, Et) were reported in 1983 [13,14]. However, the reaction of Cp_2TiCl_2 with $LiPR_2$ (R = Et, Ph) yielded the diamagnetic Ti(III) dimers $[Cp_2Ti(\mu\text{-}PR_2)]_2$ [15], evidently due to reduction of Ti(IV) by $LiPR_2$.

The reaction between $Cp(Cp^B)TiCl_2$ and one equivalent $LiPPh_2$ in toluene did not give rise to a dramatic colour change but was accompanied by the precipitation of LiCl (Scheme 3). The product, $Cp(Cp^B)Ti(PPh_2)Cl$ (**4**), was isolated by crystallisation from toluene solution. The red colour indicated that titanium had not been reduced, and indeed **4** is diamagnetic. The presence of a single resonance in the ^{31}P-NMR spectrum and the expected chlorine analysis suggest that **4** is a monomeric titanocene(IV) phosphido chloride. The ^{11}B resonances at δ −8.9 indicate a tetrahedral environment at boron, and together with the broadened ^{31}P-NMR signal this leads us to propose a Cp–B–P–Ti chelate formation. Apparently, the interaction of the phosphide ligand with boron prevents reduction of the metal centre and facilitates the isolation of the first titanocene(IV) phosphide.

The structure of **4** was determined by X-ray diffraction. There are two independent molecules in the unit cell; one is well resolved and is shown in Fig. 3, the other shows disorder with alternative sites for the Cl and Cp ligands with 50% occupancy at each site. The metal centre has a distorted tetrahedral geometry. The structure confirms the presence of a Cp–B–P–Ti chelate ring, with Cp^B(centroid)–Ti–P angles for the two molecules of 92.7° and 93.9°. In comparison, the Cp^B(centroid)–Ti–Cl angle is wider, 108.4°. The B–P distances of 2.054(4) and 2.066(4) Å are slightly longer than the corresponding bond in $(C_6F_5)_3B(PH_2CMe_3)$ (2.015(3) and 2.034(3) Å for two independent molecules) [23]. The Ti–Cl bond length is as expected for titanocene

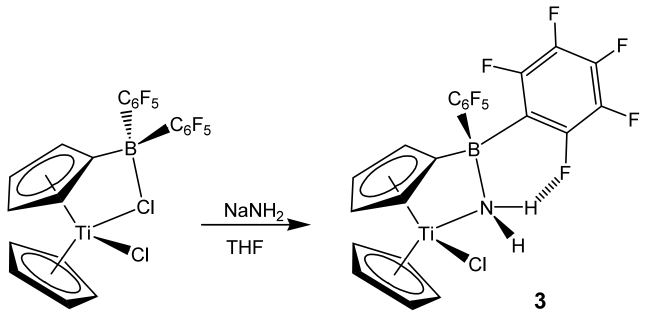

Scheme 2.

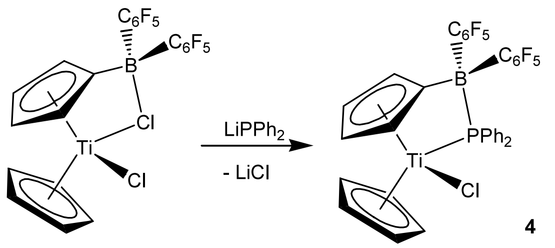

Scheme 3.

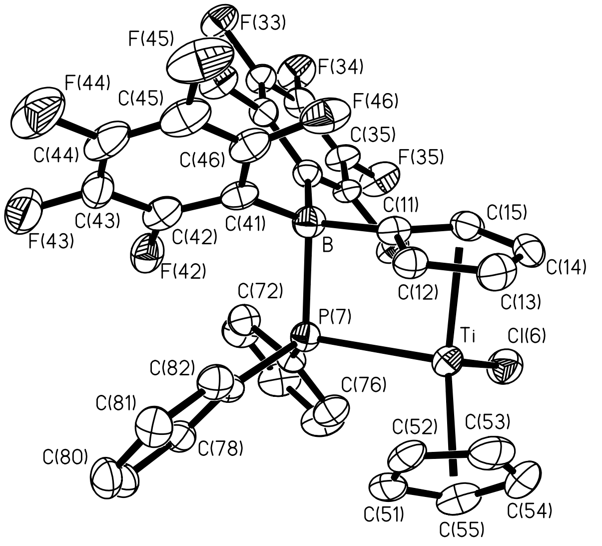

Fig. 3. Molecular structure of $Cp(Cp^B)(\mu\text{-}PPh_2)TiCl$ (**4**). Thermal ellipsoids are drawn at 50% probability. The asymmetric unit consists of two molecules; the fully ordered one of these is shown selected bond lengths (Å) and angles (°): Ti–Cl 2.320(2), Ti–P 2.6522(13), B–P 2.054(4), Ti–Cp^B(centroid) 2.051 Å, Ti–Cp(centroid) 2.074(4) Å, B–C(11) 1.635(5), B–C(31) 1.647(6), Cl–Ti–P 100.20(5), Ti–P–B 92.90(13), Cp^B(centroid)–Ti–P 92.7°.

chlorides, 2.320(2) Å. The Ti–P bond lengths of 2.6522(13) and 2.6563(13) Å compare well with the corresponding bonds in $Cp_2Ti(PPh_2)(PMe_3)$ (2.681(3) Å) and $[Cp_2Ti(PPh_2)_2]^-$ (2.67(1) and 2.71(1) Å) [15]. The structure is consistent with a Ti–P σ-bond and a P → B donor interaction, while the bond length distribution in related titanium complexes with B–N, B–Cl and B–O linkages was slightly in favour of a B-heteroatom σ-bond, with dative bonding to the metal [2]. The C(11)–Ti–P angle of 62.24(9)° is slightly more acute than the corresponding angles in **II** and its μ-OH analogue [2,4].

The existence of persistent NH···F hydrogen bonding in complexes **1**–**3** led us to look for similar, possibly unrecognised cases. A great number of Lewis base adducts of $B(C_6F_5)_3$ have been reported [16,17]. The contribution of C–F···HN bonding to the structure of the anion $[NH_2\{B(C_6F_5)_3\}_2]^-$ has been discussed above. In order to determine whether hydrogen bonding would also play a role in neutral compounds, we have examined the complexes of $B(C_6F_5)_3$ with NH_2CMe_3 and $NHMe_2$, to form primary (**5**) and secondary (**6**) amine adducts (Scheme 4). Complexation was confirmed by the ^{11}B-NMR resonances at δ −5.2 (**5**) and −1.4 (**6**), which are typical for four-coordinate neutral adducts.

Comparison of **5** with complex **1** suggests a more complex hydrogen bonding arrangement in the former, due to the presence of the third C_6F_5 substituent. The variable-temperature ^{19}F-NMR spectra of **5** are shown in Fig. 4. One broad *o*-F resonance (δ −134.6) is observed at room temperature. Cooling to −40 °C results in decoalescence into three *o*-F peaks with an integral ratio of 2:2:2. The *o*-F signal at δ −136.7 is high-field shifted due to an interaction with an N–H hydrogen atom. Cooling below −60 °C sees a further splitting of the high-field *o*-F peak. This is consistent with the structure in Scheme 4 which has two *o*-Fs

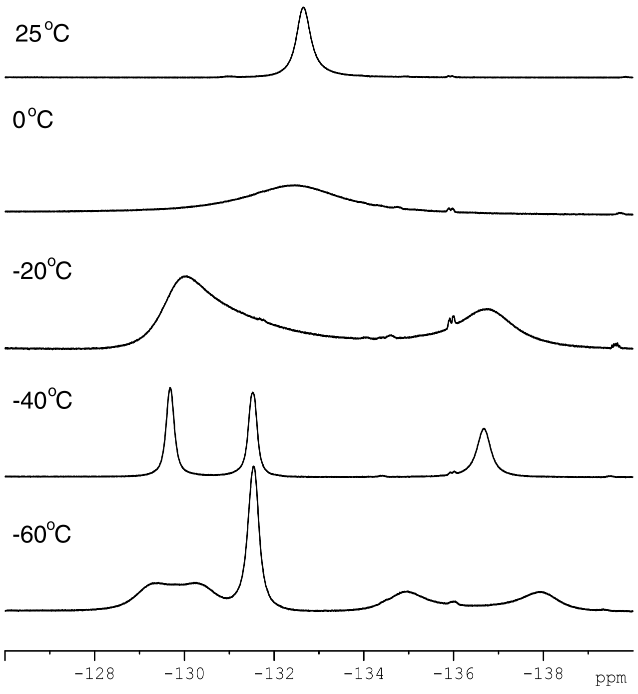

Fig. 4. Temperature dependence of the ^{19}F VT-NMR spectrum of **5**, O–F.

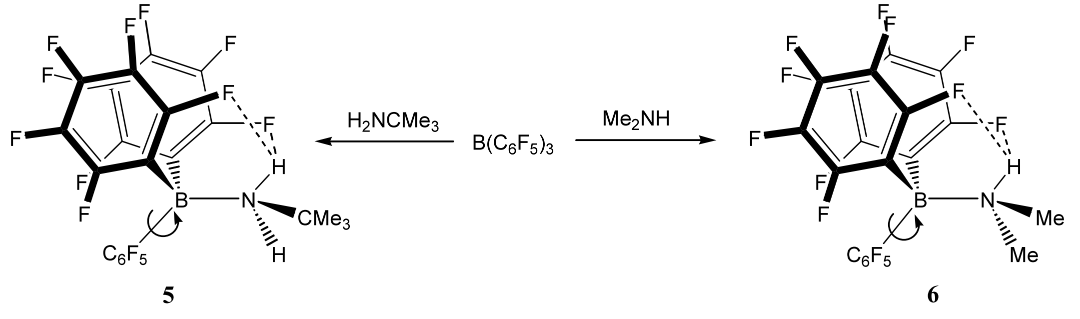

Scheme 4.

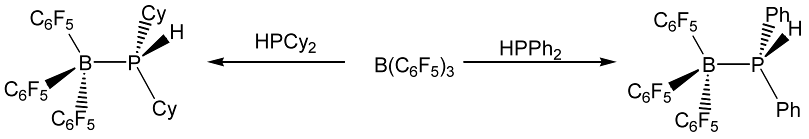

10 **11**

Scheme 5.

interacting with a single N–H, which renders the nitrogen chiral and the two C_6F_5 groups diastereotopic.

The ^{19}F-NMR spectrum of **6** at room temperature closely resembles that of **5** at −40 °C, i.e. hydrogen-bonding in **6** is even stronger. This is indicated by hindered rotation and a high-field shift for two *o*-F atoms at 20 °C of δ −142.2.

Some time ago we reported the *t*-butylamine complexes (Flu)B(C_6F_5)$_2$(NH_2CMe_3) (**7**) [1] and [(Cp^{B}NH$_2$CMe$_3$)Ti(μ-Cl)(μ-NCMe$_3$)]$_2$ (**8**) [4] (Chart 2). A reinvestigation of the crystal structures showed that in both cases at least one short N–H···F–C interaction was present, with N–H–F angles of about 130°. The ^{19}F-NMR data for **7** and **8**, as well as those for the indenylborane analogue (Ind)B(C_6F_5)$_2$(NH_2CMe_3) (**9**) [1], show broad *o*-F resonances at room temperature, while cooling to −40 °C leads to complex spectra with characteristic high-field *o*-F shifts (Table 1). The structure of **8** is also noteworthy because the second N–H engages in intramolecular hydrogen-bonding to the chloride ligand, with a short NH–Cl distance of 2.29 Å. Similar NH···Cl hydrogen-bonding interactions have been reported, for example, for the *sec*-amine titanium complexes Ti(NR)Cl$_2$(NHMe$_2$)$_2$ (R = ^{i}Pr, C_6H_5) [18].

The overriding picture that emerges is that in amine adducts of pentafluoroaryl boranes, borates and boryl-Cp complexes, hydrogen bonding between C–F bonds and amine-hydrogen atoms significantly contributes to bonding and provides the reason for strongly hindered aryl rotation which, in some cases, persists even at room temperature. In these cases, at least, organic fluorine does form strong hydrogen bonds. This point is reinforced by the observation that the *tert*-amine adduct B(C_6F_5)$_3$(MeNEt$_2$), which is bulkier than **6** but not capable of hydrogen bonding, shows no sign of hindered rotation even on cooling to −60 °C.

This situation may be compared with O–H···F–C hydrogen bonding in pentafluorophenyl Group 13 compounds. OH···F hydrogen-bonding is found in the hydrate B(C_6F_5)$_3$(OH$_2$) [19], in the anion [(C_6F_5)$_3$B(H_3O_2)B(C_6F_5)$_3$]$^-$ [20] and in (C_6F_5)$_3$Al(OH$_2$) [21], but is absent in [(C_6F_5)$_3$B(OH)B(C_6F_5)$_3$]$^-$ [22], (Cp^B)CpTi(μ-OH)Cl [4], or in the adducts B(C_6F_5)$_3$(OH$_2$)·OHCMe$_3$ and B(C_6F_5)$_3$(MeOH)·MeOH [17]. The latter is closely related to the amine adducts **5** and **6**, and the absence of F···H interactions in this compounds is therefore somewhat surprising.

In view of the strong tendency for N–H···F–C interactions in amine complexes of B(C_6F_5)$_2$X, the question arose whether hydrogen bonding was also relevant for P–H bonds. Bradley has reported a number of PH$_3$ and H$_2$PCMe$_3$ adducts of fluorinated tris(phenyl)boranes, including the crystal structure of (C_6F_5)$_3$B(PH$_2$CMe$_3$). In those examples both inter- and intra-molecular hydrogen-bonding interactions were observed, although the intramolecular H···F distance of 2.33–2.35 Å place them at the borderline of the Dunitz criteria [23]. The crystal structure of (C_6F_5)$_3$B(PH$_2$Ph) was published very recently but, by contrast, no P–H···F–C interaction was described [24]. Our analysis of the data indicates that the shortest P–H···F distance is long, 2.40 Å, and is associated with an acute P–H–F angle of 99°; therefore, it should not be regarded as a significant interaction.

The reactions between B(C_6F_5)$_3$ and the secondary phosphines PHCy$_2$ and PHPh$_2$ gave the colourless crystalline adducts, (C_6F_5)$_3$B(PHCy$_2$) (**10**) and (C_6F_5)$_3$B(PHPh$_2$) (**11**) (Scheme 5). The P–H signals in

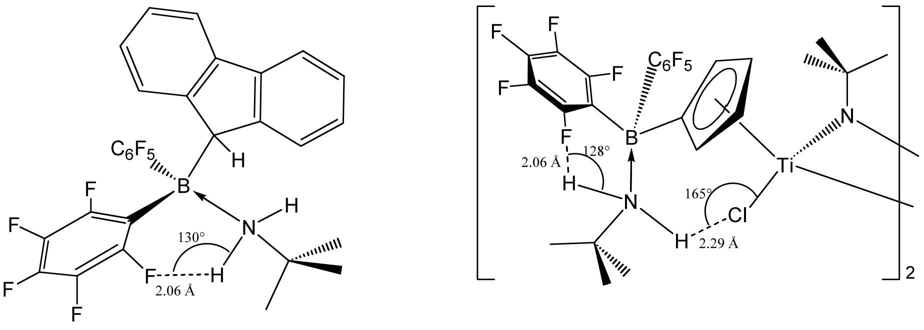

7 **8**

Plate 2.

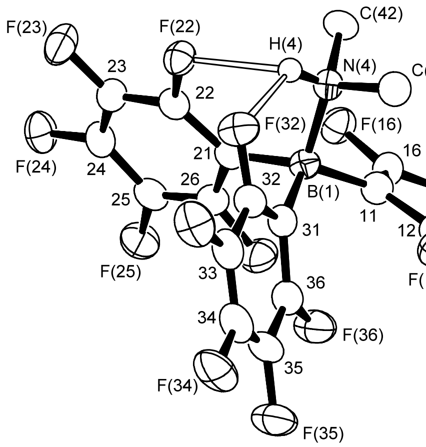

Fig. 5. Structure of $B(C_6F_5)_3(NHMe_2)$ (**6**), showing the atomic numbering scheme. Ellipsoids are drawn at 50% probability. Selected bond lengths (Å) and angles (°) for one of the two essentially identical molecules: B–N 1.653(4), B–C(11) 1.647(5), B–C(21) 1.655(4), B–C(31) 1.658(5), N–H 0.91, H–F(22) 2.15, N···F(22) 2.755(3), H–F(32) 2.10, N···F(32) 2.751(4), C(11)–B–C(21) 113.4(3), C(11)–B–C(31) 115.3(3), C(11)–B–N 103.9(2), C(21)–B–C(31) 105.7(3), N–H–F(22) 123, N–H–F(32) 128.

the ^1H-NMR spectra of the free phosphines are shifted by δ 2.34 (**10**) and 1.49 (**11**) on coordination to $B(C_6F_5)_3$. Adduct formation is also indicated by the ^{11}B chemical shifts of δ −9.4 and −13.5, respectively. The ^{19}F-NMR spectra presented no evidence for solution-phase P–H···F–C interactions.

The crystal structures of **6** and **10** are shown in Figs. 5 and 6, respectively. The bonding description based on the spectroscopic parameters is supported by the solid-state structure of **6**. There are two independent molecules in the crystal; they have essentially identical molecular conformations but lie in different orientations in the cell. The amino-hydrogen is ca. 2.1 Å from two *o*-F atoms and is involved in a bifurcated, intramolecular F···H···F hydrogen bonding system. There are also some short H···F contacts between the methyl H-atoms and F atoms of neighbouring molecules, although none are shorter than 2.42 Å. The most significant packing arrangements involve the ring of C(31–36). Firstly, this ring lies approximately parallel to, and overlapping with, the ring of C(71–76) of the second molecule, at a distance of 3.43 Å. Secondly, F(34) points directly into the centre of the C(61–66) ring of the same neighbouring molecule. The perpendicular distance of F(34) from the ring plane is 2.993(3) Å, while the six F(34)···C distances are in the range 3.191(4)–3.390(4) Å.

In **10**, the boron atom is tetrahedrally coordinated as expected. There is no indication for PH···F close contacts. The P–H and B–P bond lengths refine to 1.273(15) and 2.0270(14) Å, respectively; the latter is rather shorter than the B–P distance in **4** of 2.054(4) Å. There are no very short H···F contacts in this structure; the shortest are H(1)···F(12) and H(1)···F(36) at 2.40 and 2.46 Å, both intramolecular. H(46a)···F(35′) is the shortest intermolecular contact at 2.55 Å, i.e. at a typical van der Waals distance.

The principal packing feature between molecules is the strong interaction of F(23) with the C(11–16) ring of a neighbouring molecule; the six F···C distances are in the range of 3.143(2)–3.374(2) Å. There are no overlapping aromatic rings.

3. Conclusion

The interaction of Lewis acidic borylcyclopentadienyl ligands with donor anions E^- leads to intramolecular Cp–B–E chelate formation. Whereas zirconium complexes do not show this structural feature if E = Cl, in contrast to their Ti analogues, now it could be shown that stable complexes with an *ansa*-Cp–B–E–Zr arrangement are formed if $E = NHCMe_3$. By the same route complexes with $Cp–B–PR_2$ ligands are also accessible, as shown here in the first structurally characterised example of a Ti(IV) phosphido complex.

Hydrogen-bonding between N–H and *o*-F atoms of C_6F_5 groups is a frequent feature, both in amido-bridged *ansa*-metallocene complexes and in amine adducts of $B(C_6F_5)_3$. In some cases these intramolecular interactions are sufficiently strong to persist in solution even at room temperature and may allow H···F coupling to be observed. Hydrogen-bonding has a

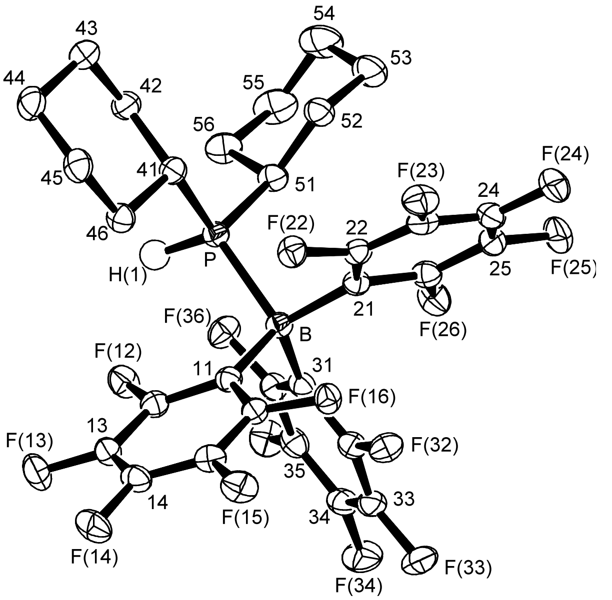

Fig. 6. Molecular structure of $B(C_6F_5)_3(PHCy_2)$ (**10**), showing the atomic numbering scheme. Hydrogen atoms of the cyclohexyl groups have been omitted for clarity. Ellipsoids are drawn at 50% probability. Selected bond lengths (Å) and angles (°): B–P 2.0270(14), B–C(11) 1.6533(18), B–C(21) 1.6484(18), B–C(31) 1.6490(18), P–H 1.273(15), P–C(41) 1.8460(13), P–C(51) 1.8441(13), C(11)–B–C(21) 115.79(10), C(11)–B–C(31) 103.91(10), C(11)–B–P 111.24(8), C(21)–B–C(31) 111.81(10), C(21)–B–P 102.40(8), B–P–H 112.7(7).

formative influence on molecular geometry and dynamics and is particularly strong where two fluorines connect to a single N–H functionality, to give a C–F···H···F–C arrangement as in **6**. Although weak hydrogen bonding to *prim*-phosphines has been reported, the *sec*-phosphine-B$(C_6F_5)_3$ adducts studied here do not show any such interaction.

4. Experimental

4.1. General procedures

All manipulations were performed under a dinitrogen atmosphere using standard Schlenk techniques. Solvents were distilled under N_2 over sodium (toluene), sodium/benzophenone (diethyl ether, tetrahydrofuran), Na/K alloy (light petroleum (bp 40–60 °C)) or CaH_2 (dichloromethane). NMR solvents (C_6D_6, CD_2Cl_2, $CDCl_3$ and $C_6D_5CD_3$) were dried over 4 Å molecular sieves and degassed by several freeze-thaw cycles. NMR spectra were recorded on a Bruker Avance DPX300 spectrometer. Chemical shifts are reported in ppm and referenced to residual solvent resonances (^{1}H, ^{13}C) or external $BF_3 \cdot OEt_2$ (^{11}B) and $CFCl_3$ (^{19}F). PPh_2H, PCy_2H (Strem) and NMe_2H (Fluka) were used as supplied, H_2NCMe_3 was dried over activated 4 Å molecular sieves. The complexes Cp$\{C_5H_4B(C_6F_5)_2\}TiCl_2$ and Cp$\{C_5H_4B(C_6F_5)_2 \cdot SMe_2\}ZrCl_2$ were prepared according to literature procedures [4]. The syntheses of **1** [4], **7** [4], **8** [4], and **9** [1] have been reported previously.

4.2. $\{C_5H_4B(C_6F_5)_2\}CpZr(Cl)(\mu\text{-}NHCMe_3)$ (2)

A solution of $\{C_5H_4B(C_6F_5)_2 \cdot SMe_2\}CpZrCl_2$ (0.75 g, 1.07 mmol) in toluene (10 cm^3) was cooled to −78 °C and solid $LiNCMe_3H$ (0.084 g, 1.07 mmol) was added. Warming to room temperature and stirring for 30 min gave a pale yellow solution and a small amount of fine precipitate. Stirring was continued for a further 2 h before the solids were allowed to settle and separated by filtration. The product was isolated by concentrating the solution to 3 ml and adding 10 ml light petroleum to precipitate a fine off-white solid (0.6 g, 0.89 mmol, 83%). Anal. Found: C, 47.00; H, 2.97; N, 2.02; Cl, 4.90%; Calc. for $C_{26}H_{19}BClNF_{10}Zr$: C, 46.41; H, 2.85; N, 2.08; Cl, 5.27%.

4.3. $\{C_5H_4B(C_6F_5)_2\}CpTi(Cl)(\mu\text{-}NH_2) \cdot 0.33(C_7H_8)$ (3)

To a solution of $\{C_5H_4B(C_6F_5)_2\}CpTiCl_2$ (1.15 g, 1.94 mmol) in tetrahydrofuran (20 ml) $NaNH_2$ (0.076 g, 1.94 mmol) was added. The reaction was followed by ^{1}H-NMR and was complete after stirring at room temperature for 36 h. The solvent was removed and the product extracted with 10 cm^3 toluene. Cooling to −25 °C overnight gave red crystals, which retained ca. 0.33 equivalents of toluene even after drying under vacuum (0.7 g, 1.16 mmol, 60%). Anal. Found: C, 47.86; H, 2.06; N, 2.05%; Calc. for $C_{24.31}H_{13.64}BClF_{10}NTi$: C, 48.35; H, 2.28; N, 2.32%.

4.4. $\{C_5H_4B(C_6F_5)_2\}CpTi(Cl)(\mu\text{-}PPh_2)$ (4)

A solution of $\{C_5H_4B(C_6F_5)_2\}CpTiCl_2$ (1.44 g, 2.43 mmol) in toluene (50 ml) was cooled to −78 °C and solid $LiPPh_2$ (0.47 g, 2.43 mmol) was added. Slow warming to room temperature and stirring for 30 min gave a deep red solution and a small amount of fine precipitate. Stirring was continued for a further 2 h before the solid was allowed to settle and separated by filtration. Removal of the solvent under reduced pressure gave a red solid which was recrystallised from dichloromethane and light petroleum affording red crystals suitable for X-ray crystallography, yield 1.01 g, 1.45 mmol, 56%. Anal. Found: C, 54.17; H, 2.69; Cl, 5.75%. Calc. for $C_{34}H_{19}BClF_{10}P$: C, 54.99; H, 2.58; Cl, 4.77%.

4.5. $(C_6F_5)_3B(NH_2CMe_3)$ (5)

The compound was prepared by mixing a solution of $B(C_6F_5)_3$ (2.65 g, 5.2 mmol) in 30 ml toluene with NH_2CMe_3 (20.7 ml of a 0.25 M solution in toluene) and isolated as colourless crystals (2.56 g, 82.6%). Anal. Found: C, 45.52; H, 1.86; N, 2.40%. Calc. for $C_{20}H_7BF_{15}N$: C, 45.16; H, 1.90; N, 2.39%.

4.6. $(C_6F_5)_3B(NHMe_2)$ (6)

This compound was made from $B(C_6F_5)_3$ (3.74 g, 7.3 mmol) and NMe_2H (7.3 mmol, 3.03 ml of a 2.41 M solution in toluene) and isolated as colourless crystals after recrystallisation from a light petroleum/dichloromethane mixture (3.21 g, 79%). Anal. Found: C, 43.08; H, 1.11; N, 2.55%. Calc. for $C_{20}H_7BF_{15}N$: C, 43.12; H, 1.27; N, 2.51%.

4.7. $(C_6F_5)_3B(PHCy_2)$ (10)

In a similar procedure to **5**, from $B(C_6F_5)_3$ (0.76 g, 1.5 mmol) and PCy_2H (0.30 ml, 1.6 mmol) and isolated as colourless crystals after recrystallisation from a light petroleum/dichloromethane mixture (0.91 g, 85%). Anal. Found: C, 51.34; H, 3.54%. Calc. for $C_{30}H_{23}BF_{15}P$: C, 50.73; H, 3.26%.

Table 2
Crystal data for compounds **4**, **6** and **10**

Compound	**4**	**6**	**10**
Empirical formula	$C_{34}H_{19}BClF_{10}PTi$	$C_{20}H_7BF_{15}N$	$C_{30}H_{23}BF_{15}P$
fw	742.6	557.1	710.3
Crystal system	triclinic	monoclinic	monoclinic
Space group	$P\bar{1}$ (No. 2)	Cc (No. 9)	$P2_1/n$ (equiv. to no. 14)
a (Å)	10.073(2)	14.910(3)	11.666(1)
b (Å)	12.807(3)	15.423(3)	12.077(1)
c (Å)	23.750(5)	19.373(4)	20.562(1)
α (°)	78.75(3)	90	90
β (°)	86.57(3)	112.50(3)	96.052(3)
γ (°)	87.93(3)	90	90
V, (Å^{-3})	2998.7(10)	4116.1(14)	2880.8(4)
Z	4	8	4
D_{calc} (g cm^{-3})	1.645	1.798	1.638
μ, mm^{-1}	0.517	0.201	0.215
$F(0\,0\,0)$	1488	2192	1432
θ Range (°)	$1.6 \leq \theta \leq 25.4$	$2.0 \leq \theta \leq 25.4$	$1.9 \leq \theta \leq 26.4$
Index range	$-11 \leq h \leq 11$, $-14 \leq k \leq 15$, $-28 \leq l \leq 28$	$-17 \leq h \leq 17$, $-17 \leq k \leq 18$, $-23 \leq l \leq 23$	$-14 \leq h \leq 14$, $0 \leq k \leq 15$, $0 \leq l \leq 25$
No. of reflections collected/unique/observed	15 085/9399/5199 ($R_{int} = 0.059$)	11 941/7013/5649 ($R_{int} = 0.072$)	32 362/5887/5426 ($R_{int} = 0.023$)
Data/restraints/parameters	9399/0/914	7013/2/667	5887/0/428
Goodness of fit on F^2, S	0.860	0.959	1.032
R_1 [$I > 2\sigma(I)$]	0.043	0.038	0.032
wR_2 (all data)	0.093	0.091	0.086
Weighting parameters a, b	0.0102, 0	0.0313, 0	0.0469, 1.14
Largest difference peak and hole e Å^{-3}	0.30 and −0.34	0.20 and −0.18	0.34 and −0.23

Definitions: $R_{int} = (\Sigma|F_o^2 - F_c^2 \text{ (mean)}|/\Sigma F_o^2)$; $S = [(\Sigma w(F_o^2 - F_c^2)^2)/(n-p)]^{1/2}$; $wR_2 = [\Sigma w(F_o^2 - F_c^2)^2/\Sigma w(F_o^2)^2]^{1/2}$; $R_1 = (\Sigma||F_o| - |F_c||/\Sigma|F_o|)$; weighting scheme $w = [\sigma^2(F_o^2) + (aP)^2 + bP]^{-1}$, where $P = [2F_c^2 + \max(F_o^2, 0)]/3$.

4.8. $(C_6F_5)_3B(PHPh_2)$ (**11**)

To a solution of $B(C_6F_5)_3$ (1.24 g, 2.4 mmol) in toluene (50 ml) was added PPh_2H (0.45 ml, 2.4 mmol). The solution was stirred for 1 h before removal of the solvent in vacuo. The crude product was recrystallised from a light petroleum/dichloromethane mixture at −25 °C affording colourless, needle-shaped crystals (1.31 g, 84%). Anal. Found: C, 50.85; H, 1.41%. Calc. for $C_{30}H_{13}BF_{15}P$: C, 51.61; H, 1.59%.

4.9. X-ray crystallography

The analytical procedures were similar for the three samples. Crystal and refinement data are collated in Table 2. For each, a crystal was mounted in oil on a glass fibre and fixed in the cold nitrogen stream. Intensity data for complexes **4** and **6** were measured on a Rigaku R-Axis IIc image plate diffractometer equipped with a rotating anode X-ray source (Mo–K_α radiation) and graphite monochromator; the data were processed with the DENZO/SCALEPACK programs [25]. Complex **10** was measured on a Bruker Smart APEX CCD instrument and processed using the SAINT [26] programs and corrected with SADABS [27]. All data were measured at 140 K. The structure of each was determined by the direct methods routines in the SHELXS program [28] and refined by full-matrix least-squares methods, on F^2s, in SHELXL [28]. In general, the non-hydrogen atoms were refined with anisotropic thermal parameters. Hydrogen atoms were included in idealised positions and their U_{iso} values were set to ride on the U_{eq} values of the parent nitrogen and carbon atoms. Scattering factors for neutral atoms were taken from Ref.[29]. Computer programs used in these analyses were run on a Silicon Graphics Indy at the University of East Anglia, or a DEC-Alpha Station 200 4/100 in the Biological Chemistry Department, John Innes Centre.

Crystallographic data have been deposited with the Cambridge Crystallographic Data Centre, CCDC No. 210664–210666 for compounds **4**, **6** and **10**.

Acknowledgements

This work was supported by the Engineering and Physical Sciences Research Council and the University of East Anglia. We are grateful to Dr T. Wagner of Bruker AXS for measurement of the data for compound **10**.

References

[1] R. Duchateau, S.J. Lancaster, M. Thornton-Pett, M. Bochmann, Organometallics 16 (1997) 4995.

[2] M. Bochmann, S.J. Lancaster, G. Jiménez Pindado, D.A. Walker, S. Al-Benna, M. Thornton-Pett, in: M.G. Davidson, A.K. Hughes, T.B. Marder, K. Wade (Eds.), Contemporary Boron Chemistry, Royal Society of Chemistry, London, 2000, p. 10.

[3] M.T. Reetz, H. Brümmer, M. Kessler, J. Kuhnigk, Chimia 49 (1995) 501.

[4] S.J. Lancaster, S. Al-Benna, M. Thornton-Pett, M. Bochmann, Organometallics 19 (2000) 1599.

[5] S.J. Lancaster, D.L. Hughes, J. Chem. Soc. Dalton Trans. (2003) 1779.

[6] (a) J.D. Dunitz, R. Taylor, Chem. Eur. J. 3 (1997) 89;
(b) V.R. Thalladi, H.C. Weiss, D. Bläser, R. Boese, A. Nangia, G.R. Desiraju, J. Am. Chem. Soc. 120 (1998) 8702.

[7] (a) T.J. Barbarich, C.D. Rithner, S.M. Miller, O.P. Anderson, S.H. Strauss, J. Am. Chem. Soc. 121 (1999) 4280;
(b) U. Diederichsen, Angew. Chem. Int. Ed. 37 (1998) 1655.

[8] (a) S. Moran, R.X.F. Ren, S. Rumney, IV, E.T. Kool, J. Am. Chem. Soc. 119 (1997) 2056;
(b) T.A. Evans, K.R. Seddon, Chem. Commun. (1997) 2023.

[9] (a) B. Temme, G. Erker, J. Karl, H. Luftmann, R. Fröhlich, S. Kotila, Angew. Chem. Int. Ed. Engl. 34 (1995) 1755;
(b) J. Ruwwe, G. Erker, R. Fröhlich, Angew. Chem. Int. Ed. Engl. 35 (1996) 80;
(c) J. Karl, G. Erker, R. Fröhlich, J. Am. Chem. Soc. 119 (1997) 11165;
(d) G. Erker, Acc. Chem. Res. 34 (2001) 309.

[10] (a) G. Jiménez Pindado, M. Thornton-Pett, M. Bouwkamp, A. Meetsma, B. Hessen, M. Bochmann, Angew. Chem. Int. Ed. Engl. 36 (1997) 2358;
(b) S.J. Lancaster, M. Thornton-Pett, D.M. Dawson, M. Bochmann, Organometallics 31 (1998) 3829;
(c) T.J. Woodman, M. Thornton-Pett, M. Bochmann, Chem. Commun. (2001) 329;
(d) T.J. Woodman, M. Thornton-Pett, D.L. Hughes, M. Bochmann, Organometallics 20 (2001) 4080.

[11] S.J. Lancaster, A. Rodriguez, A. Lara-Sanchez, M.D. Hannant, D.A. Walker, D.L. Hughes, M. Bochmann, Organometallics 21 (2002) 451.

[12] (a) K. Kunz, G. Erker, S. Döring, R. Fröhlich, G. Kehr, J. Am. Chem. Soc. 123 (2001) 6181;
(b) G. Altenhoff, S. Bredeau, G. Erker, G. Kehr, O. Kataeva, R. Fröhlich, Organometallics 21 (2002) 4084.

[13] R.T. Baker, J.F. Whitney, S.S. Wreford, Organometallics 2 (1983) 1049.

[14] D.W. Stephan, Angew. Chem. Int. Ed. 39 (2000) 314.

[15] D.G. Dick, D.W. Stephan, Organometallics 10 (1991) 2811.

[16] See for example: (a) A.G. Massey, A.J. Park, F.G.A. Stone, Proc. Chem. Soc., (1963) 212;
(b) A.G. Massey, A.J. Park, J. Organomet. Chem. 2 (1964) 245;
(c) M.J.G. Lesley, A. Woodward, N.J. Taylor, T.B. Marder, I. Cazenobe, I. Ledoux, J. Zyss, A. Thornton, D.W. Bruce, A.K. Kakkar, Chem. Mater. 10 (1998) 1355;
(d) H. Jacobsen, H. Berke, S. Döring, G. Kehr, G. Erker, R. Fröhlich, O. Meyer, Organometallics, 18 (1999) 1724;
(e) M.A. Beckett, D.S. Brassington, M.E. Light, M.B. Hursthouse, J. Chem. Soc. Dalton Trans. (2001) 1768;
(f) J.M. Blackwell, W.E. Piers, M. Parvez, R. McDonald, Organometallics 21 (2002) 1400;
(g) J.M. Stoddard, K.J. Shea, Organometallics 23 (2003) 1124.

[17] C. Bergquist, B.M. Bridgewater, C.J. Harlan, J.R. Norton, R. Friesner, G. Parkin, J. Am. Chem. Soc. 122 (2000) 10581.

[18] (a) N. Adams, A.R. Cowley, S.R. Dubberley, A.J. Sealey, M.E.G. Skinner, P. Mountford, Chem. Commun. (2001) 2738;
(b) G. Aullón, D. Bellamy, L. Brammer, E.A. Bruton, A.G. Orpen, Chem. Commun. (1998) 653.

[19] L.H. Doerrer, M.L.H. Green, J. Chem. Soc. Dalton Trans. (1999) 4325.

[20] M.J. Drewitt, M. Niedermann, M.C. Baird, Inorg. Chim. Acta 340 (2002) 207.

[21] D. Chakraborty, E.Y.-X. Chen, Organometallics 22 (2003) 207.

[22] A.A. Danopoulos, J.R. Galsworthy, M.L.H. Green, S. Cafferkey, L.H. Doerrer, M.B. Hursthouse, Chem. Commun. (1998) 2529.

[23] D.C. Bradley, I.S. Harding, A.D. Keefe, M. Motevalli, D.H. Zheng, J. Chem. Soc. Dalton Trans. (1996) 3931.

[24] J.-M. Denis, H. Forintos, H. Szelke, L. Toupet, T.-N. Pham, P.-J. Madec, A.-C. Gaumont, Chem. Commun. (2003) 54.

[25] Z. Otwinowski, W. Minor, Meth. Enzymol. Part A 276 (1997) 307.

[26] R.A. Sparks, SAINT—Area-detector Software Package, Bruker AXS, Madison, Wisconsin, 1995.

[27] G.M. Sheldrick, SADABS—Program for Empirical Absorption Correction of Area-Detector Data, University of Göttingen, Germany, 1996.

[28] G.M. Sheldrick, SHELX-97—Programs for Crystal Structure Determination (SHELXS) and Refinement (SHELXL), University of Göttingen, Germany, 1997.

[29] International Tables for X-ray Crystallography, Kluwer Academic, Dordrecht, vol. C, (1992) pp. 500, 219 and 193.